Effect of the environment on the performance of GFRP reinforcing bars

T. D'Antino*, M.A. Pisani, C. Poggi

Department of Architecture, Built Environment and Construction Engineering, Politecnico di Milano, Piazza Leonardo da Vinci 32, 20133, Milan, Italy

Fiber reinforced Polymer (FRP) composites are currently employed in the civil engineering industry as externally bonded reinforcement (EBR) of existing reinforced concrete (RC) and masonry structures and as internal re-inforcement of concrete elements as an alternative to steel reinforcing bars. Carbon FRP (CFRP) composites are mainly used for EBR applications whereas glass FRP (GFRP) bars are employed as internal reinforcement of concrete elements. This paper sheds light into the effect of different aggressive environments on the tensile behavior of reinforcing GFRP bars. 356 results of tensile tests of GFRP bars subjected to hot dry and humid air, different alkali environments, salt solutions with various concentrations, and plain and distillated water were collected from the literature. According to the "design by testing" procedure provided by EN 1990, a statistical analysis of the results was carried out to calibrate environmental reduction factors able to provide reliable estimations of the long-term behavior of GFRP bars subjected to different exposure conditions. For a given aggressive environment, a clear and unique degradation trend could not be identified, which points out the need of a standard testing procedure able to provide reliable and repeatable results.

Keywords: Glass fibers, Environmental degradation, Mechanical properties, GFRP bars, Environmental reduction factor

1. Introduction

In cold regions de-icing is traditionally done with salt along with sand and gravel. Salt is the most efficient de-icing agent if the pavement temperature is not below −18 °C. Moreover, it is cheap, easy to spread and store, and readily available in large quantities. Nevertheless, the use of de-icing salt on bridge decks leads to corrosion of steel reinforcing bars and therefore affects their durability. The corrosion of steel reinforcing bars causes cracking and spalling of concrete bridge decks with consequent elevated costs for rehabilitation and traffic disruption. To overcome these issues, from the early nineties Glass Fiber Reinforced Polymer (GFRP) bars have been adopted in some regions like Canada as internal reinforcement of concrete slabs, increasing their service life in these unfavorable conditions (see e.g. Refs. [1–3]). GFRP bars, which are comprised of glass fibers embedded within organic matrices, have a high strength-to-weight ratio and a good durability with respect to certain exposure conditions. Moreover, GFRP bars are particularly suitable as internal reinforcement of concrete bridge decks because they show good resistance to fatigue loads [4]. Because of these properties, fiber reinforced composites have been increasingly employed to strengthen existing concrete elements [5–16].

However, GFRP bars are sensitive to some environmental conditions. In particular, alkaline environment, moisture, and extreme temperatures degrade their mechanical properties (e.g., tensile strength, ultimate strain, and modulus of elasticity) [17–21]. GFRP reinforcing bars are usually comprised of E-Glass fiber reinforcement, which is known to be degraded by marked alkaline environment. Although alkali-resistant (AR) glass fibers showed good durability to alkaline environment such as cementitious matrixes [22], their use in GFRP bars is still limited and the bar alkali-resistance is assigned to the matrix that should prevent the diffusion of deleterious ions [23]. The absorption of moisture depends on the type of organic matrix employed. Moisture, which penetrates within the matrix through a diffusion process at the molecular level, mainly affects the matrix causing plasticization, strength decrease, and reduction of the glass transition temperature value.

The elastic modulus and strength of GFRP bars decrease with increasing temperature. This behavior is mainly caused by the marked change of mechanical properties of the organic matrix when temperature attains values close or above the glass transition temperature of the matrix, whereas the glass fibers do not significantly change their properties (see for instance [24]).

Design codes and guidelines (see Refs. [23,25–27]) generally take into account the possible degradation of GFRP bars by means of a strength reduction factor η_a (known also as environmental reduction factor), whose value should depend on fiber/resin type and exposure conditions, and should be calibrated using a sufficiently large number of experimental tests.

In this paper, after a brief description of GFRP bars and their mechanical properties, 356 results of conditioned GFRP bars subjected to

Received 13 October 2017;
Received in revised form 18 December 2017;
Accepted 18 December 2017
Available online 21 December 2017

* Corresponding author.
E-mail addresses: tommaso.dantino@polimi.it (T. D'Antino), marcoandrea.pisani@polimi.it (M.A. Pisani), carlo.poggi@polimi.it (C. Poggi).

tensile tests carried out by 20 different research groups are collected from the literature and compared to assess the effect of different exposure conditions. The effect on the bar tensile strength of prolonged exposition to hot dry and humid air, alkali environment with different pH, salt solutions with different concentrations, and plain and distillated water were investigated, also considering the bar fiber volume fraction (i.e. ratio between the fiber volume and volume of the bar) and matrix and resin type. Results were divided in groups depending on the exposure time and temperature. According to the "design by testing" procedure provided by EN 1990, a statistical analysis of the results was carried out to calibrate environmental reduction factors able to provide reliable estimations of the long-term behavior of GFRP bars subjected to different exposure conditions. The results obtained help to shed light on the durability of GFRP bars with respect to different exposure and accelerated aging conditions. However, it is opinion of the authors that further studies are needed to obtain reliable estimations of the long-term behavior of GFRP bars.

2. GFRP reinforcing bars

GFRP reinforcing bars are comprised of longitudinal glass fibers impregnated with an organic resin. The tensile strength and modulus of elasticity of GFRP bars, which are affected by several factors (e.g. fiber volume fraction, typically ranging between 0.5 and 0.7, and manufacturing and curing conditions), were reported to vary between 483 MPa and 1600 MPa and between 35 GPa and 51 GPa, respectively [23]. To improve the bond behavior between the GFRP reinforcing bar and the embedding concrete, different bar surfaces can be employed. Although smooth bars are available (usually with small diameters), the bar surface may be molded-deformed with resin ribs, ribbed with glass fiber wrapped around the bar longitudinal axis, sand-coated, or may present a combination of these treatments.

2.1. Tensile tests

The experimental evaluation of the tensile strength of GFRP bars is not an easy task due to the difficulty to anchor the specimen to the testing machine. The reason of this difficulty is the marked orthotropy of this unidirectionally-reinforced composite material. The GFRP bar weakness in radial direction requires a soft gripping of the specimen but, at the same time, a strong gripping is needed to allow for attaining rupture of the glass fibers. Anchor heads are often used to provide the proper stress-transfer from the testing machine to the specimen without damaging the bar [28]. GFRP bars tested in tension can present different failure modes:

- ***Tensile rupture.*** This failure mode is associated with the highest stress that can be attained. The failure occurs with a sudden contemporary collapse of all fibers and an extensive interfacial debonding while the broken fibers are fan-shaped (Fig. 1);
- ***Slippage at the bar-anchor head interface.*** The anchorage is not effective and the bar slips with respect to the machine wedge or to the anchor head (Fig. 2);
- ***Fiber trimming on the collar of the anchor area.*** The edges of the anchor head (or the machine wedges) cut the peripherals fibers of the bar at the loaded end, where the interface pressure has a peak [28] (Fig. 3);
- ***Longitudinal delamination.*** Non-uniform radial pressure distribution causes detachment of portions of the bar at the bar-anchor head interface, where the contact pressure is low. As a consequence, bar delamination in the direction parallel to the fibers occurs (Fig. 4).

Fig. 1. Fiber tensile rupture at the end of a tensile test.

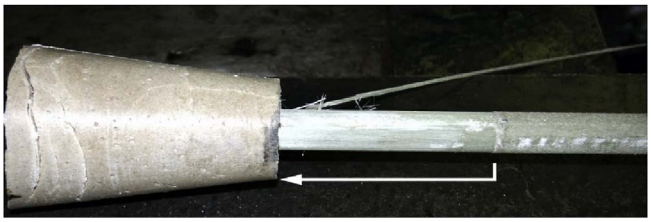

Fig. 2. Slippage at the bar-anchor head interface.

Fig. 3. Failure due to fiber trimming on the collar of the anchor area.

To obtain the complete tensile rupture of the bar, ASTM D7205 [29] recommends anchorages comprised of steel tubes filled with either a polymer resin or an expansive cement grout able to prevent excessive slip of the bar prior to failure. The recommended steel tube length varies from 300 mm to 460 mm for GFRP bars with diameter that varies between 6.4 mm and 9.5 mm.

2.2. Long-term behavior tests

To investigate the long-term behavior of GFRP bars subjected do different exposure conditions, accelerated aging tests are usually adopted. No specific standard or guideline for accelerated tests of GFRP bars is currently available and only a standard general framework for developing accelerated tests for building materials and components is available from the literature [30]. Different models for estimating the long-term behavior of GFRP bars can be found in the literature [31]. However, GFRP accelerated aging tests are generally based on the Arrhenius equation, which provides the relation between the analyzed reaction rate (e.g. diffusion of humidity within the matrix resin) and the temperature:

$$k = Ae^{-E_a/RT} \tag{1}$$

where k is the reaction rate constant, A is the pre-exponential factor that depends on the type of reaction, E_a is the activation energy of the reaction, and R and T are the universal gas constant and absolute temperature, respectively. Coefficients of Eq. (1) can be calibrated following the procedures provided by ASTM E 2041 [32] and ASTM E 698 [33]. Arrhenius equation assumes that there is a single dominant degradation process that does not change with time. Moreover, the process degradation rate increases with increasing temperature [34]. With these assumptions, Arrhenius equation can be employed to obtain

Fig. 4. Longitudinal delamination failure.

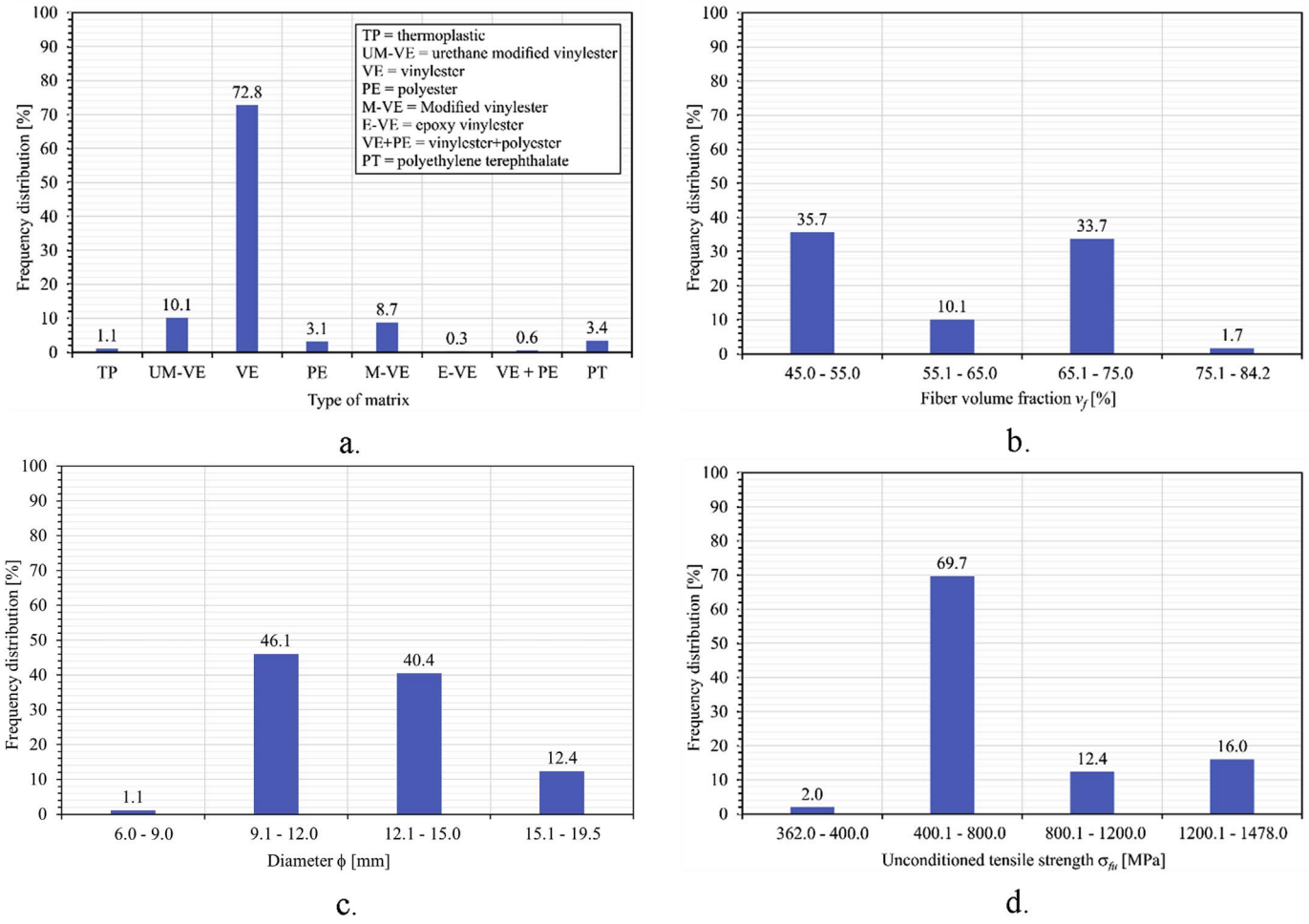

Fig. 5. Frequency distribution of a) matrix type, b) fiber volume fraction v_f, c) diameter ϕ, and d) unconditioned tensile strength σ_{fu} of bars included in the database.

the relationship between the behavior of a GFRP bar exposed to a specific aggressive condition at temperature T_1 for a time period t_1 and that of a GFRP bar exposed to the same condition at temperature $T_2 > T_1$ and for a time period $t_2 < t_1$. Therefore, the long-term behavior and service-life of GFRP bars can be investigated by increasing the temperature for a given exposure condition. The main limit of this approach lies in the assumption that the reaction process does not change with time. In fact, it was observed that reaction processes tend to change during the exposure period, which may affect the provisions obtained with the Arrhenius equation [35].

3. Experimental database

The experimental database employed in this paper is comprised of 356 results of tensile tests on conditioned GFRP bars collected from the literature. Results were obtained by 20 research groups [31,34,36–53]. In this section, the database is presented and analyzed while a detailed discussion of the results is reported in Section 5. Bars included in the database are mainly made of E-glass fibers (340 specimens, 95.5% of total specimens) although some specimens comprising alkali-resistant (AR) glass fibers (16 specimens, 4.5% of total specimens) were considered.

Specimens presented different matrix type, fiber volume fraction v_f, diameter ϕ, tensile strength of the unconditioned (control) specimen σ_{fu}, and surface treatment. Different matrix types were used, namely thermoplastic (TP), urethane modified vinylester (UM-VE), vinylester (VE), polyester (PE), modified vinylester (M-VE), epoxy vinylester (E-VE), mixed vinylester and polyester (VE + PE), and polyethylene terephthalate (PT). The fiber volume fraction v_f ranged between 45.0 and 84.2 (according to the authors), whereas the bar diameter ϕ ranged between 6.0 mm and 19.5 mm.

The initial (unconditioned) tensile strength σ_{fu} of the bar varied between 362 MPa and 1478 MPa. The frequency distribution of specimens included in the database is depicted in Fig. 5a, b, c, and d for different matrix types and different ranges of v_f, ϕ, and σ_{fu}, respectively. Details of the specimens included in the database and subjected to hot dry and humid air, alkali environment, salt solutions, plain and distillated water, and embedded within concrete beams immersed in plain water and salt solution (sea water) are provided in the appendix in Tables A1, A2, A3, A4, and A5, respectively.

The bar surface treatment, indicated in Tables A1-A5 for each specimen, was assumed to have no influence on the bar tensile strength and was not included among the parameters studied.

4. Analysis and comparison of conditioned GFRP bar residual strength

The database collected was employed to evaluate the effect on GFRP bar tensile strength of prolonged exposition to:

I) hot dry and humid air,
II) alkali environment with different pH,
III) salt solutions with different concentrations,
IV) plain and distillated water.

Results are provided in term of residual strength ratio σ_f/σ_{fu}, which

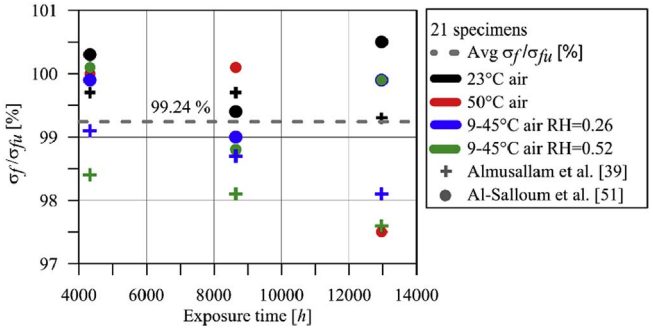

Fig. 6. Residual strength ratio of bars exposed to air with various temperatures and RH for different exposure times.

is defined as the ratio between the tensile strength of the conditioned specimen σ_f and the tensile strength σ_{fu} of the corresponding unconditioned specimen.

4.1. Bars exposed to hot air with different relative humidity

Two research groups investigated the residual strength of GFRP bars exposed to air for different exposure times. Twelve specimens [51] were comprised of bare GFRP bars, whereas 9 specimens were comprised of GFRP bars embedded within a concrete prism in their central part [50]. All bars employed were comprised of E-glass fiber and vinylester matrix (Table A1). Two exposure temperatures were considered, namely 23 °C (lab conditions) and 50 °C. Some specimens were exposed to two different field conditions with temperatures in the range 9–45 °C and average relative humidity RH = 0.26 and RH = 0.52.

The residual strength ratio σ_f/σ_{fu} obtained for each specimen is shown in Fig. 6. The results show that exposure to air did not significantly affect the bar strength (minimum residual strength ratio σ_f/σ_{fu} = 97.5% for a bar exposed to 50 °C air for 12960 h). Since a small scatter between results is observed (coefficient of variation CoV = 0.90%), the average residual strength ratio σ_f/σ_{fu} = 99.24% could be computed without distinguishing between different exposure times. Furthermore, a clear influence of the RH cannot be observed. Specimens conditioned within concrete provided results similar to those obtained with bare bars, which indicated that the well-known concrete alkalinity did not affect the bar residual strength ratio [50]. This observation is not always confirmed by tests on bars subjected to different alkaline environment, as discussed below.

4.2. Bars immersed in alkaline solutions with different pH

202 specimens were tested by 18 research groups to investigate the effect of different alkaline environments on the bar tensile strength. Bars were mainly comprised of E-glass fibers with different volume fraction and vinylester matrix, although some bars presented different resin matrix (e.g. thermoplastic, urethane, polyester). Eight bars comprised of AR-glass and different inorganic matrices [37] were considered for comparison. Details of each bar, including the diameter and surface treatment, are provided in Table A2. To simulate a harsh alkaline environment, specimens were immersed in alkaline solutions that were heated to accelerate the degradation process. The alkaline solutions adopted were grouped in four pH ranges, namely pH = 12–12.15, pH = 12.5–12.7, pH = 13, and pH = 13.4–13.6. Similarly, the solution temperatures were divided in three ranges, namely range *a* (11–25 °C), *b* (26–53 °C), and *c* (57–80 °C). The residual strength ratio of each conditioned bar is shown in Fig. 7 for the different temperature ranges analyzed. The results reported in Ref. [38] were not considered because specimens were embedded in concrete and the pH was not clearly measured. Robert et al. [49] and Robert and Benmokrane [52] conditioned bars embedded in concrete and measured the pH of the interstitial solution extracted from concrete after aging. Similarly, Almusallam et al. [50] conditioned bars embedded within concrete with pH between 12.5 and 13 (pH = 12.7 was assumed). Specimens subjected to freeze and thaw and wet and dry cycles were not considered for comparison.

Bars subjected to different alkaline environments in the temperature range 11–25 °C (66 specimens, Fig. 7a), show a decreasing residual strength ratio with increasing the exposure time. Data with pH = 13.0 and pH = 13.4–13.6 show a decrease rate much higher than those with pH = 12–12.15 and pH = 12.5–12.7. These results, however, are affected by the failure mode of the bar. Considering Almusallam et al. [50] and Vijay [31], which attained complete bar failure, it is possible to observe a minimum residual strength ratio of 78.3%. Results from Al-

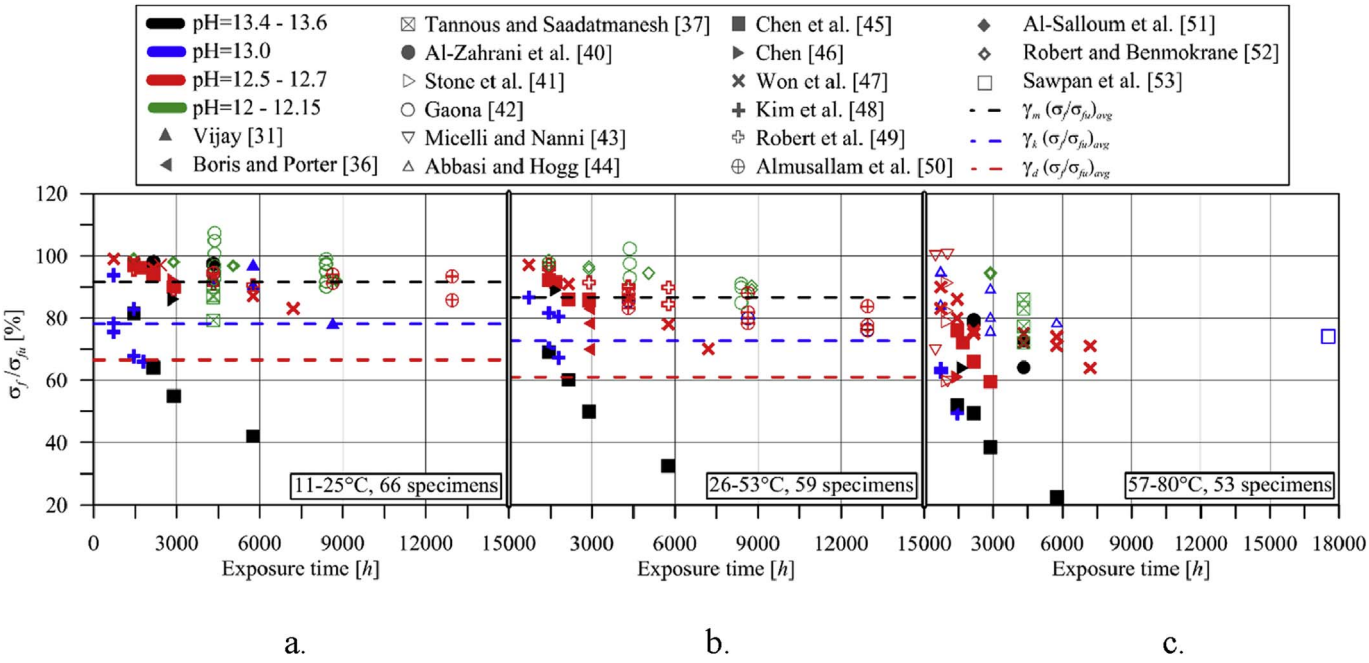

Fig. 7. Residual strength ratio of bars exposed to alkaline solutions at a) 11–25 °C, b) 26–53 °C, and c) 57–80 °C for different exposure times.

Zahrani et al. [40], which tested bars similar to those employed by Vijay [31] under a more aggressive exposure condition, did not show a significant strength reduction. This difference may be attributed to the slippage of the bars within the anchorage, which prevented the fiber failure of specimens by Al-Zahrani et al. [40].

Although the behavior of results by Chen et al. [45] and Chen [46] is in agreement with the behavior generally observed for increasing value of pH, a minimum residual strength ratio (σ_f/σ_{fu} = 42.0% for 5760 h exposure and pH = 13.6) lower than that reported for the same conditioning time and similar pH values (σ_f/σ_{fu} = 90.9% for 5760 h exposure and pH = 13.0, Vijay [31]) was observed. This difference could be attributed to the non-complete bar failure observed in Refs. [45,46], which reported bar delamination with partial fiber tensile failure.

Considering specimens that were subjected to different alkaline environments at temperatures in the range 26–53 °C (59 specimens), it is possible to observe a general decrease of the bar residual strength ratio for increasing exposure time and pH (Fig. 7b). For authors that documented a complete bar failure, i.e. tensile rupture of all fibers within the cross-section [49–52], a minimum residual strength ratio of 76.0% was observed, which is similar to that observed for specimens subject to temperatures in the range 11–25 °C. This suggests that the temperature range considered did not significantly affect the bar tensile strength. Analogously to specimens conditioned at 11–25 °C, the results from Refs. [45,46] presented a larger strength decrease rate for specimens subjected to pH = 13.5 than those subjected to pH = 12.5–12.7, with a minimum residual strength ratio of 32.5% for 5760 h exposure and pH = 13.5.

Boris and Porter [36] tested bars with different matrices (two bars with a mixed vinylester-polyester matrix and one bar with a vinylester matrix) subjected to the same environment (pH = 12.7) for 2904 h. Their results showed that the vinylester matrix provided a better protection to the bar, which had a residual strength ratio of 83.1%, whereas bars with the mixed vinylester-polyester matrix showed an average residual strength ratio of 74.1%. However, this consideration cannot be generalized because the number of specimens tested appears too limited.

Considering the temperature range 57–80 °C (Fig. 7c), 53 specimens were exposed to different alkali environments and presented a significant decrease of residual strength ratio with increasing exposure time. Various authors reported different behaviors and different residual strength ratio decrease rates with time t, $d(\sigma_f/\sigma_{fu})/dt$. Robert and Benmokrane [52], which reported complete bar failure, observed a limited strength decrease, namely σ_f/σ_{fu} = 94.4%, for a bar conditioned for 2880 h. Chen et al. [45] reported a clear decreasing behavior, with increasing $d(\sigma_f/\sigma_{fu})/dt$ with increasing pH. Won et al. [47] reported a lower $d(\sigma_f/\sigma_{fu})/dt$ respect to that observed by Chen et al. [45] for the same pH and exposure time. Micelli and Nanni [43] tested different diameter bars and observed that a significant strength decrease occurred for bars with diameter 6.3 mm, whereas no decrease was observed for bars with diameter 12 mm. Surprisingly, the bar tested by Sawpan et al. [53] after 17520 h exposure with pH = 13.0 reported a residual strength ratio higher than that reported by other authors for lower pH and exposure time.

Specimens comprising AR-glass provided σ_f/σ_{fu} values similar to those of specimens made of E-glass conditioned for the same exposure time and temperature. However, no final conclusions can be drawn since this result was attributed to the specific AR-glass bar manufacturing process and tests with different bars were suggested by the authors to confirm the results [37].

Results of specimens comprising different fiber volume fractions v_f and conditioned for different exposure times are shown in Fig. 8 for the three temperature ranges considered. For bars in the range 11–25 °C (Fig. 8a), a clear influence of v_f on the residual strength ratio cannot be observed. High residual strength ratios were obtained with fiber volume fractions higher or equal to 60% and lower than 50%, whereas scattered results were obtained for v_f = 50%.

The fiber volume fraction v_f appears to have a limited effect on the residual strength ratio for bars conditioned at 26–53 °C. Similar residual strength ratio values were obtained for bars with v_f higher than 70% conditioned for the same number of hours [49]. However, a slight reduction of the bar residual strength ratio for high values of v_f (namely 84.2%), was observed (Fig. 8b).

For bars with 49.1% ≤ v_f ≤ 60%, the fiber volume fraction appeared to affect the bar tensile strength. A reduction of residual strength ratio from σ_f/σ_{fu} = 83.1% to σ_f/σ_{fu} = 69.9% was reported by Boris and Porter [36] for bars with v_f = 54.3% and v_f = 58.3%, respectively, which were conditioned for 2904 h. Similarly, Kim et al. [48] observed

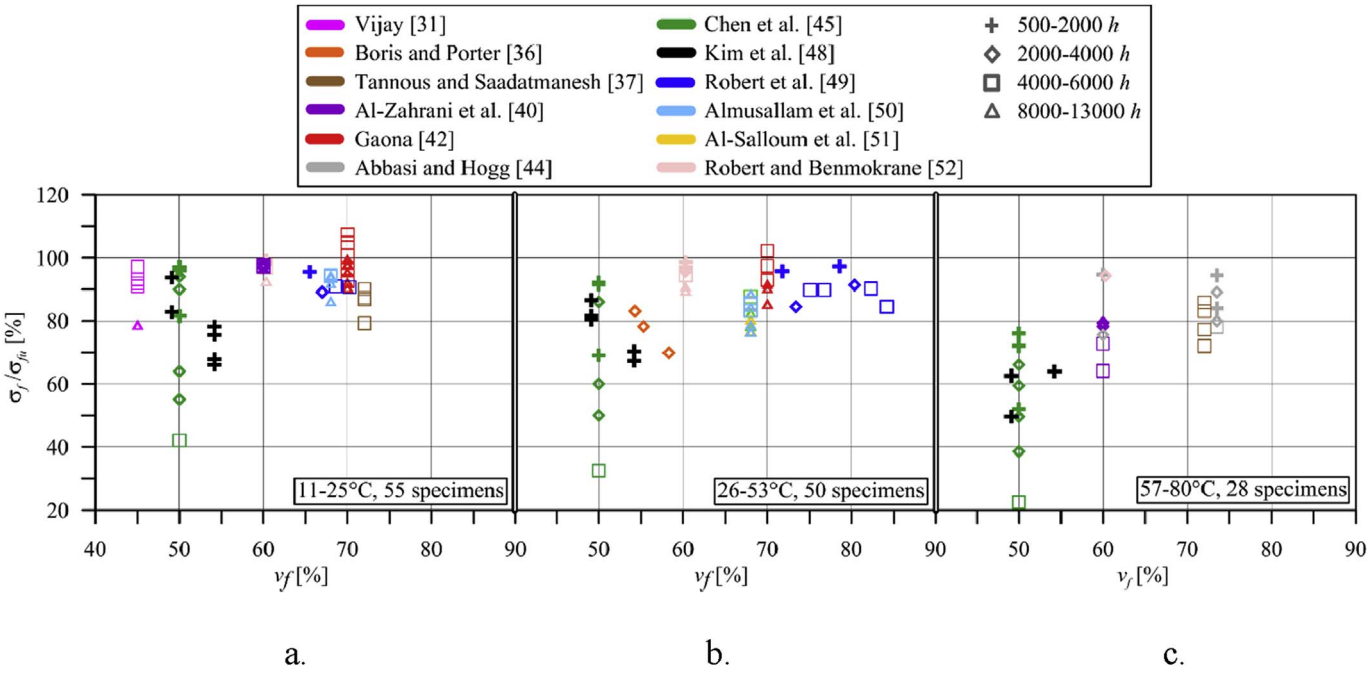

Fig. 8. Residual strength ratio of bars exposed to alkaline solutions at a) 11–25 °C, b) 26–53 °C, and c) 57–80 °C for different fiber volume fractions.

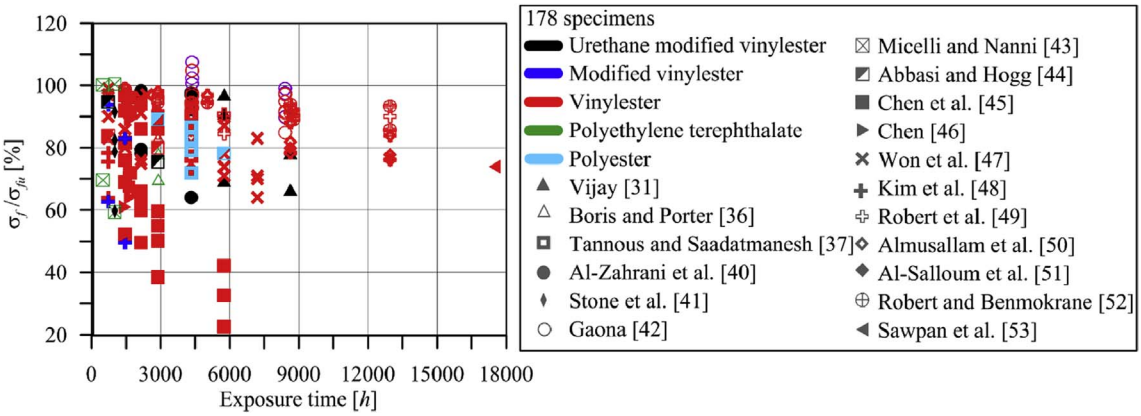

Fig. 9. Residual strength ratio of bars comprising different matrix types exposed to alkaline solutions for different exposure times.

a strength reduction from 80.5% to 67.3% for bars conditioned for 1800 h and with v_f = 49.9% and v_f = 54.2%, respectively.

Comparing the residual strength ratio obtained by bars with different fiber volume fractions conditioned at temperatures in the range 57–80 °C, the ratio σ_f/σ_{fu} appears to increase with increasing v_f (Fig. 8c). This behavior, which is in contrast with the behavior observed for specimens conditioned at temperatures between 26 °C and 53 °C that showed an opposite trend, could be explained by the matrix severe degradation at temperatures close to the glass transition temperature, which in turn could have affected the residual strength ratio of bars with low fiber volume fraction.

Since bars comprising AR-glass had the same fiber volume fraction v_f = 72.0%, the influence of v_f on the residual strength ratio obtained could not be investigated.

All specimens subjected to alkaline environment are shown in Fig. 9 for different exposure times and with the indication of the matrix type employed. The scatter between the results obtained do not allow for identifying the effect of each matrix type. It should be noted, however, that most specimens (73%) were made of vinylester resin.

The average of residual strength ratios for each temperature range considered, together with the corresponding coefficient of variation and number of specimens considered, are reported in Table 1. A decrease of the residual strength ratio with increasing temperature can be observed, with a minimum average residual strength ratio of 73.2% for the temperature range 57–80 °C. If related to the temperature of exposure, this result shows a relatively limited bar degradation.

The computation of the average of residual strength ratio made in Table 1 are based on the outcomes of Fig. 9, which do not show a dependence of the residual strength ratio on the exposure time, although such relationship should be reasonably expected.

4.3. Bars immersed in solutions with different salt concentrations

Results of 47 GFRP bars immersed in solutions with different salt concentrations were collected from the literature. Four bars were subjected to freeze and thaw cycles and were not considered for comparison [31]. Most of the bars were comprised of E-glass fiber and vinylester matrix and presented a ribbed surface with sand coating. Details of each bar are provided in Table A3. The bars were immersed in saline solutions heated to accelerate the degradation process. Three temperature ranges were identified, namely range *a* (11–25 °C), *b* (40–50 °C), and *c* (80 °C). Furthermore, different salt concentrations were considered, namely 3% by weight, 3.5% by weight, and ≥4% by weight. To obtain the last salt concentration, sea water of the Arabian Gulf-Eastern Province of Saudi Arabia, which can have a salt concentration even higher than 4% by weight (see for instance [54–56]), was employed.

Twenty-one bars were immersed in salt solutions at 11–25 °C. The degradation obtained was not pronounced and the residual strength ratio was higher than 80% except for one bar conditioned for 7200 h that provided a residual strength ratio of 74.8% (Fig. 10a). For this temperature range, the salt concentration did not appear to influence the results, which do not present a clear trend.

Results from 14 specimens conditioned at 40–50 °C (Fig. 10b) show a limited reduction of tensile strength, with a minimum residual strength ratio of 77.2% associated with 1440 h conditioning. Four specimens were also subjected to wet and dry cycles (WD in Fig. 10), which did not affect the residual strength ratio obtained.

Only one research group applied a conditioning temperature higher than 50 °C, namely Kim et al. [48], which conditioned 8 specimens at 80 °C (Fig. 10c). The results obtained show two separate groups, the former with residual strength ratios between 80.7% and 89.7% and the latter with residual strength ratios between 42.6% and 65.3%. The presence of two distinct groups can be attributed to the different matrix type and fiber volume fraction of the bars, as discussed below.

The fiber volume fraction v_f does not seem to affect the bar residual strength ratio for specimens conditioned at 11–25 °C (Fig. 11a), whereas σ_f/σ_{fu} shows a slight increase with increasing v_f for specimens conditioned at 40–50 °C (Fig. 11b). A significant increase of residual strength ratio was observed for bars conditioned at 80 °C with increasing v_f from 49.1% to 54.2% (Fig. 11c).

All specimens subjected to saline environment are shown in Fig. 12 for different exposure times and with the indication of the matrix type employed. Vinylester, urethane modified vinylester and polyester matrix did not affect the obtained residual strength ratio. Specimens with modified vinylester matrix (v_f = 49.1%) conditioned at 80 °C showed a significant reduction of residual strength ratio respect to bars with vinylester matrix (v_f = 54.2%) subjected to the same conditioning. However, it should be noted that this difference shall not be entirely attributed to the matrix type but also to the different fiber volume fractions.

The average of residual strength ratios for each temperature range considered, together with the corresponding coefficient of variation and number of specimens, is reported in Table 2. The average residual strength ratio of specimens conditioned at 11–25 °C and 40–50 °C is very similar. Although a significant reduction is observed for specimens conditioned at 80 °C, the average σ_f/σ_{fu} = 68.2% cannot be confirmed

Table 1
Average residual strength ratio of bars immersed in alkaline solutions for different temperature ranges.

Range	Temperature [°C]	Number of specimens	Average σ_f/σ_{fu} [%] (CoV)
a	11–25	66	88.9 (0.139)
b	26–53	59	84.3 (0.145)
c	57–80	53	73.2 (0.205)

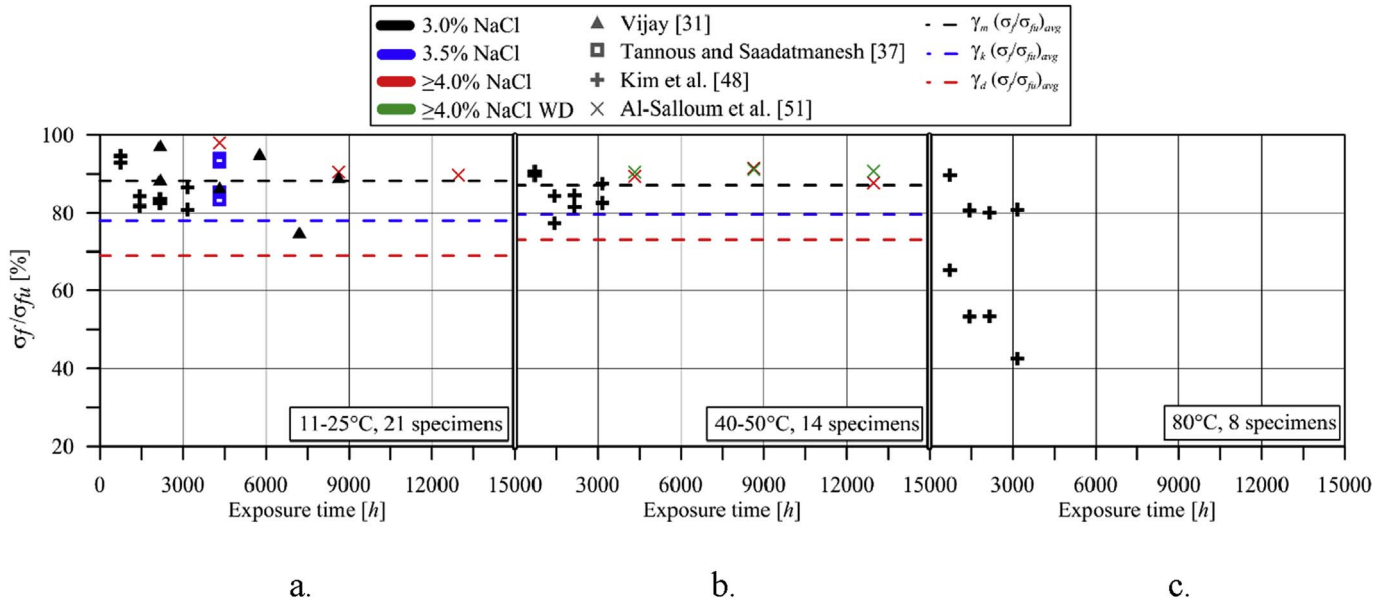

Fig. 10. Residual strength ratio of bars exposed to saline solution at a) 11–25 °C, b) 40–50 °C, and c) 80 °C for different exposure times.

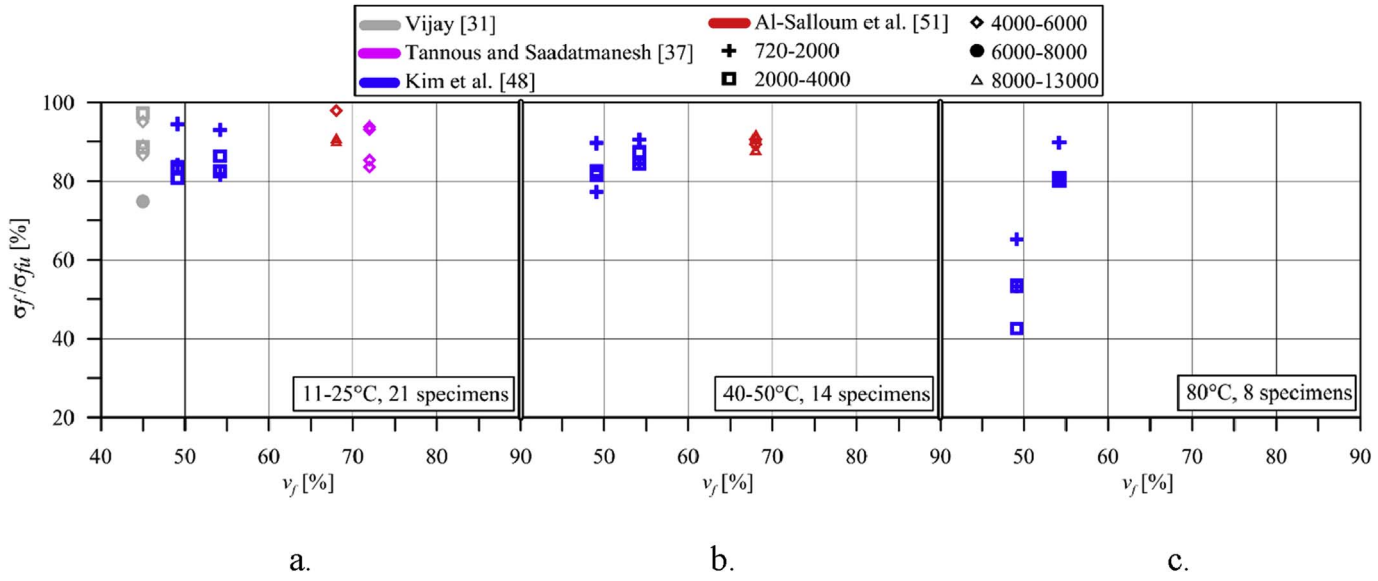

Fig. 11. Residual strength ratio of bars exposed to saline solution at a) 11–25 °C, b) 40–50 °C, and c) 80 °C for different fiber volume fractions.

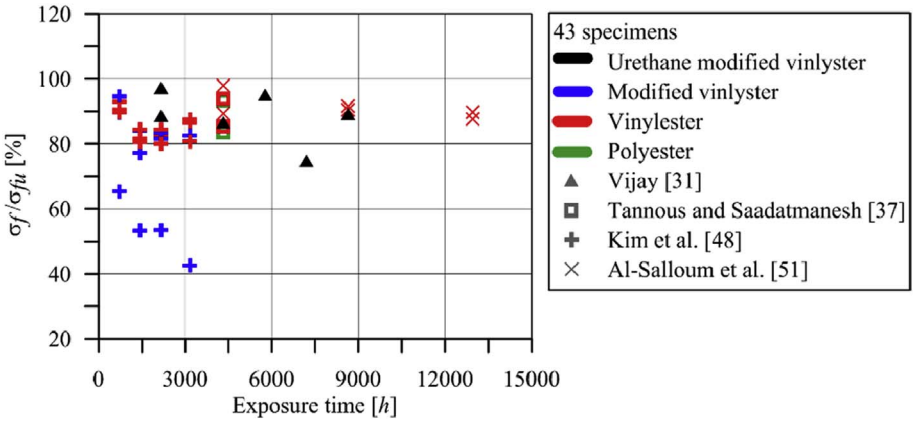

Fig. 12. Residual strength ratio of bars comprising different matrix types exposed to saline solutions for different exposure times.

Table 2
Average residual strength ratio of bars immersed in salt solutions for different temperature ranges.

Range	Temperature [°C]	Number of specimens	Average σ_f/σ_{fu} [%] (CoV)
a	11–25	21	88.2 (0.069)
b	40–50	14	87.0 (0.050)
c	80	8	68.2 (0.249)

due to the large scatter between results conditioned at 80 °C (CoV = 0.249), presence of differences between bars tested (i.e. matrix type and fiber volume fraction), and absence of results from different authors.

4.4. Bars immersed in water

Fifty-seven specimens, tested by five different research groups, were immersed in tap or distillated water for different exposure times to assess the effect of possible moisture absorption on the bar tensile strength. Bars with different matrix types and fiber volume fractions were employed (Table A4). In one case, which is not considered for comparison, wet and dry cycles were applied [46]. To accelerate the moisture absorption, the conditioning water was heated at different temperatures. Results were divided into three groups depending on the water temperature, namely range *a* (11–25 °C), *b* (26–50 °C), and *c* (60–80 °C).

Residual strength ratios of bars immersed in water at 11–25 °C, 26–50 °C, and 60–80 °C for different exposure times are reported in Fig. 13a, b, and c, respectively. For low temperatures (11–25 °C), the bar tensile strength was not significantly affected by the water conditioning. Results by Al-Salloum et al. [51], which reported a complete bar failure, showed a minimum residual strength ratio of 95.1% for 12960 h exposure time. Results by Kim et al. [48] are more scattered, with a minimum residual strength ratio of 75.7% for 1440 h exposure time. For some specimens, Gaona [42] reported an increase of tensile strength after conditioning. Differences between results by Al-Salloum et al. [51], Gaona [42], and Kim et al. [48] may be attributed to the different fiber volume fraction adopted (Fig. 14a). Indeed, the residual strength ratio appears to increase with increasing v_f in the range 11–25 °C.

Eighteen specimens were immersed in water at 26–50 °C and presented residual strength ratios like those obtained at 11–25 °C (Fig. 13b). However, specimens tested by Al-Salloum et al. [51] reported a residual strength ratio between 15% and 20% lower than that obtained by the same authors at 11–25 °C for the same exposure times. This behavior can be also observed by comparing the residual strength ratio for varying fiber volume fractions in the range 26–50 °C, where σ_f/σ_{fu} increases with increasing v_f except for specimens by Al-Salloum et al. [51] (Fig. 14b).

Nine specimens were immersed in water heated at temperatures between 60 °C and 80 °C (Fig. 13c). The residual strength ratio obtained from these specimens is generally lower than that obtained at temperature in the range 11–50 °C, with a minimum residual strength ratio σ_f/σ_{fu} = 43.9% for 3168 h exposure time. As for lower temperatures, σ_f/σ_{fu} appeared to increase with increasing v_f for specimens conditioned at 60–80 °C (Fig. 14c).

Comparing results obtained with bars made of different matrix types, a clear influence of the matrix was not observed in the range 11–50 °C (Fig. 13a and b). However, only specimens made with polyethylene terephthalate matrix presented an increase of tensile strength after conditioning [42]. For conditioning at 60–80 °C, specimens with modified vinylester matrix (v_f = 49.1%) were associated with residual strength ratios lower than those obtained with the vinylester matrix (v_f = 54.2%) for the same exposure times. This behavior, which was observed for specimen immersed in salt solution and conditioned at 80 °C by the same research group [48], should be attributed both to the matrix type and fiber volume fraction but was not confirmed by other authors.

The average of residual strength ratios for each temperature range considered, together with the corresponding coefficient of variation and number of specimens, is reported in Table 3. Specimens in ranges 11–25 °C and 26–50 °C provided similar results, although slightly lower values were obtained in the range 26–50 °C. Similarly to the case of bars immersed in salt solutions, high temperatures (60–80 °C) were associated with significant strength reduction (average σ_f/σ_{fu} = 67.2%). This behavior was observed by a single research group and could not be confirmed by other data.

4.5. Bars embedded within concrete beams immersed in plain water and salt solution (sea water)

To study the durability of GFRP bars under real serviceability conditions, some authors immersed concrete beams reinforced with GFRP bars in plain water and salt solutions. After the conditioning period, the bars were extracted from the beams and subjected to tensile test to assess their strength.

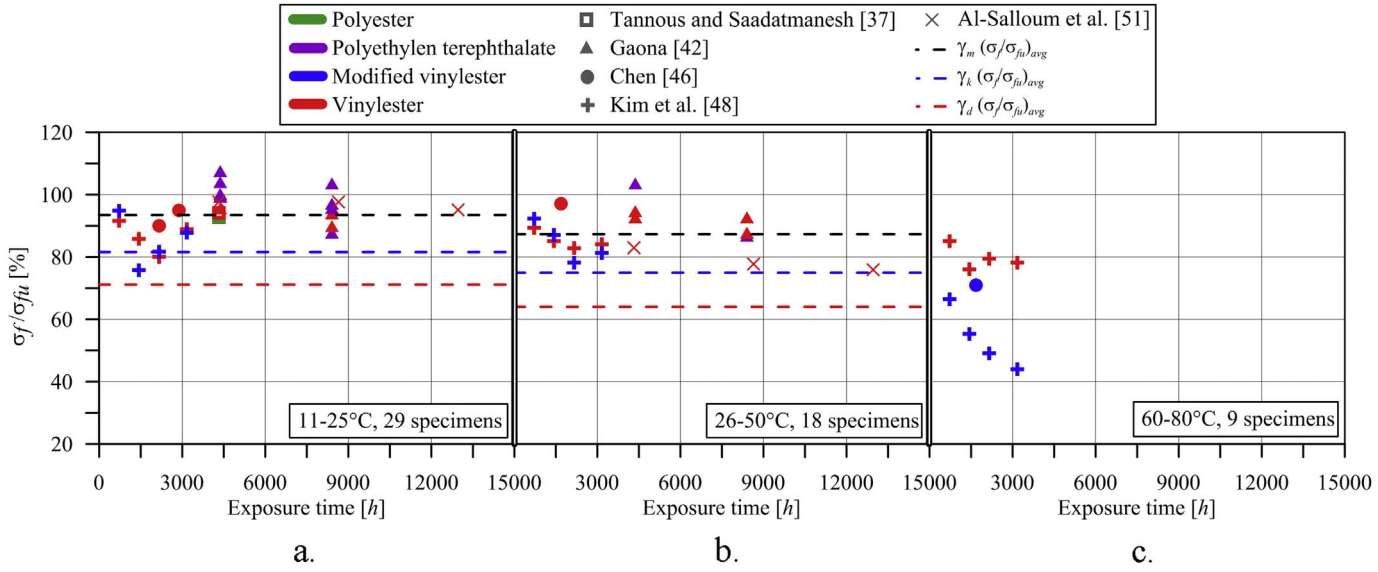

Fig. 13. Residual strength ratio of bars immersed in water at a) 11–25 °C, b) 26–50 °C, and c) 60–80 °C for different exposure times.

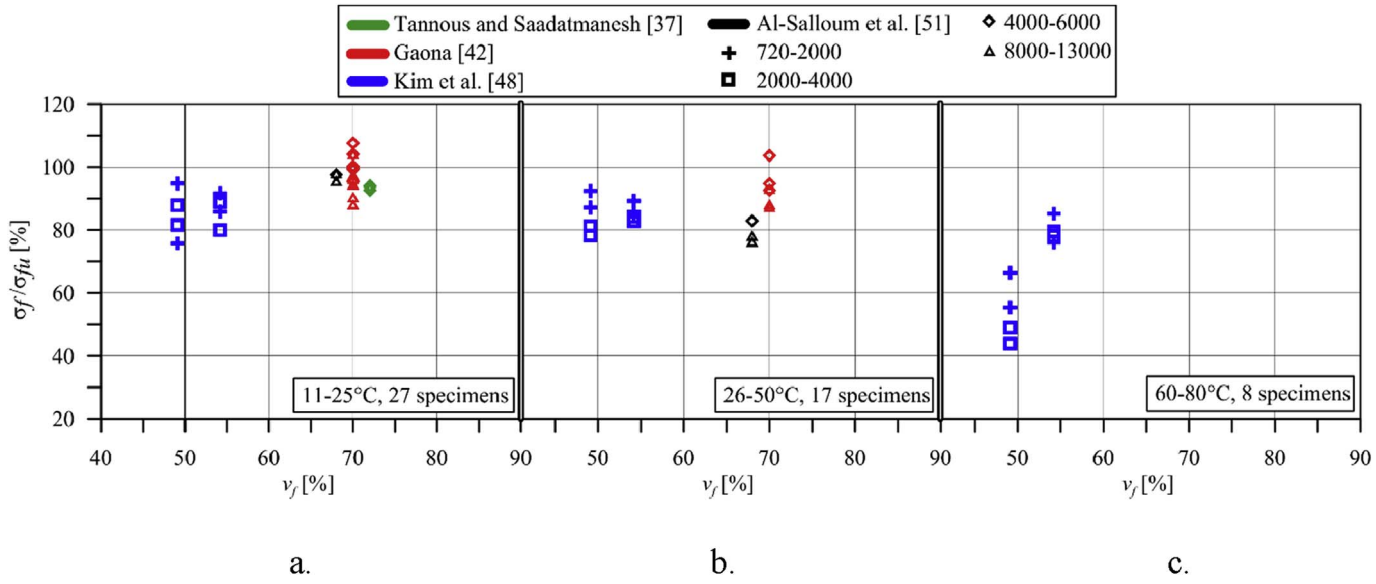

Fig. 14. Residual strength ratio of bars immersed in water at a) 11–25 °C, b) 26–50 °C, and c) 60–80 °C for different fiber volume fractions.

Table 3
Average residual strength ratio of bars immersed in water for different temperature ranges.

Range	Temperature [°C]	Number of specimens	Average σ_f/σ_{fu} [%] (CoV)
a	11–25	29	93.5 (0.076)
b	26–50	18	87.3 (0.083)
c	60–80	9	67.2 (0.217)

Twenty-nine GFRP bars comprising E-glass fiber and vinylester matrix were used as reinforcement of concrete beams that were immersed in plain water and in a salt solution for different exposure times (Table A5). For the salt solution, sea water of the Arabian Gulf-Eastern Province of Saudi Arabia, which can have a salt concentration higher than 4% by weight, was employed [39,50]. To accelerate the possible bar degradation, the conditioning water was heated at 40 °C, 50 °C, and 60 °C for some specimens.

The residual strength ratio σ_f/σ_{fu} obtained by bars conditioned at various temperatures is plotted in Fig. 15 for different exposure times. Specimens by Davalos et al. [34] showed a decrease of σ_f/σ_{fu} with increasing the exposure time. Furthermore, the rate of decrease of σ_f/σ_{fu} increased with increasing the conditioning temperature. If compared with specimens directly immersed in water (Fig. 13a), bars embedded within concrete and conditioned at 20 °C showed a similar residual strength ratio, whereas lower residual strength ratios were observed for bars embedded within concrete and conditioned at 40 °C respect to those directly immersed in water at similar temperatures (Fig. 13b). This difference may be attributed to the alkalinity of the embedding concrete that contributed to the bar degradation. Indeed, a similar residual strength ratio was obtained by bars embedded within concrete and bars directly immersed in alkaline solutions at temperatures between 11 °C and 53 °C (Fig. 7a and b). However, it should be noted that specimens embedded within concrete and exposed to air did not show a significant strength reduction ([50], Section 4.1).

When conditioned at 50–60 °C, specimens embedded within concrete showed a significant strength decrease with increasing exposure time. A similar decrease was observed for some specimens directly immersed in water at temperature in the range 60–80 °C (Fig. 13c), whereas higher residual strength ratios were provided by bars directly immersed in alkaline solutions with pH ≤ 13 at 57–80 °C (Fig. 7c).

In Fig. 15 the residual strength ratio obtained by bars embedded within concrete and conditioned with a solution with NaCl ≥ 4% by weight (≥ 4% NaCl in Fig. 15) and subjected to wet and dry cycles with the same solution (≥ 4% NaCl WD in Fig. 15) is also reported. The σ_f/σ_{fu} obtained showed that specimens conditioned with salt solution were less degraded than those conditioned with plain water at the same temperature (i.e. 40 °C). Specimens subjected to wet and dry cycles provided σ_f/σ_{fu} values lower than those of specimens simply immersed in the same salt solution but higher than those of corresponding bars conditioned with plain water.

Residual strength ratios are plotted in Fig. 16 for specimens tested at 20–40 °C with different fiber volume fractions v_f, which did not have

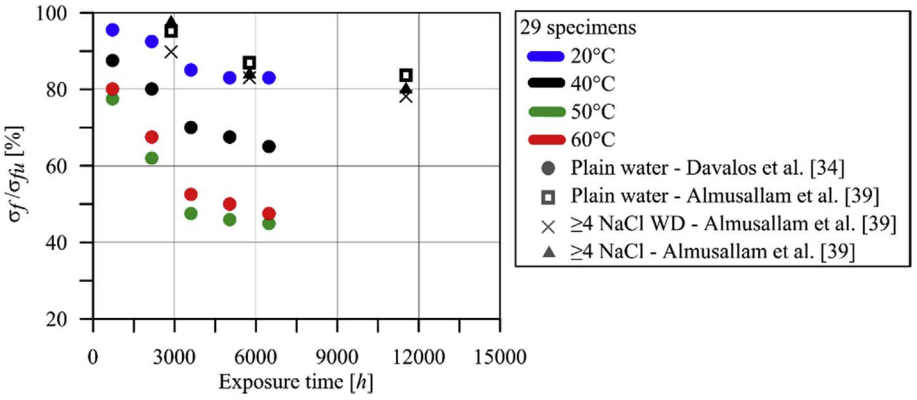

Fig. 15. Residual strength ratio of bars embedded within concrete and immersed in plain water and salt solution at 20 °C, 40 °C, 50 °C, and 60 °C for different exposure times.

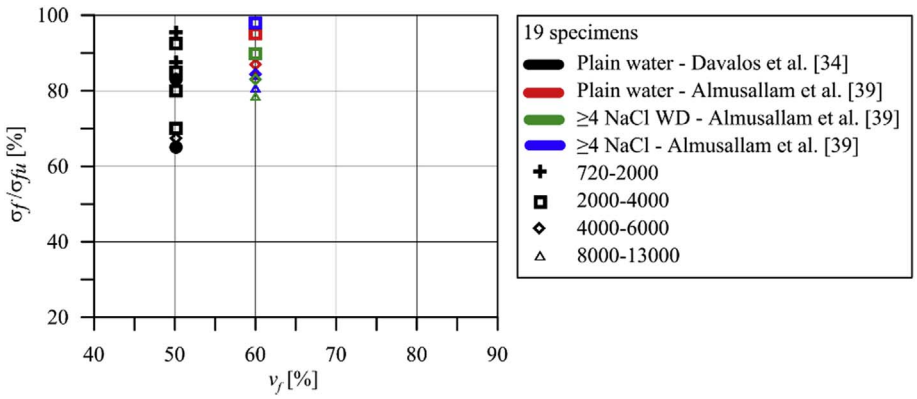

Fig. 16. Residual strength ratio of bars embedded within concrete and immersed in plain water and salt solution at 20–40 °C for different fiber volume fractions.

Table 4
Average residual strength ratio of bars embedded within concrete for different temperature ranges.

Range	Temperature [°C]	Number of specimens	Average σ_f/σ_{fu} [%] (CoV)
a	20–40	19	83.6 (0.108)
b	50–60	10	57.6 (0.231)

any influence on the results. The influence of fiber volume fraction was not studied for specimens exposed to temperature higher than 40 °C, which had the same v_f. Furthermore, since all bars were comprised of E-glass fiber and vinylester matrix, the influence of matrix and fiber type could not be investigated.

The average residual strength ratio provided by specimens embedded within concrete at 20–40 °C (range *a* in Table 4) is similar to that obtained from bars directly immersed in alkaline solutions at 26–53 °C (Table 1). However, higher conditioning temperature provided an average residual strength ratio lower for bars embedded within concrete (range *b* in Table 4) than for bars directly immersed in alkaline solutions, salt solutions, and plain water (Tables 1–3, respectively). The average results are affected by the overall number of specimens and by the number of specimens tested for each exposure time considered.

5. Discussion

The comparison of the residual tensile strength obtained from GFRP reinforcing bars exposed to severe environmental conditions and tested by 20 different research groups showed in many cases contradictory results and discordant trends.

The first issue is represented by the temperature of water solutions employed for conditioning some specimens. It is well-known that temperatures above 50 °C, although often lower than the glass transition temperature of the organic matrix, affect the physical properties of the bars by increasing the thermal expansion coefficient [57]. Therefore, the adoption of such high temperatures to accelerate the degradation process can alter the bar and should be adopted only in the case of real severe environmental conditions, since usual serviceability conditions never reach these high temperatures. In fact, the highest temperature of the sea surface is measured in the Persian Gulf, where 37 °C can be attained (see for instance [56,58]). Consequently, results of experimental tests made on bars conditioned in water solutions heated at temperatures above 40 °C are not realistic and may be affected by the modification of the GFRP properties.

The accelerated alkali environment conditions do not reflect the real exposure condition of reinforcing bars. The pH values selected for the accelerated alkaline environment conditions, which vary between 12 and 13.6 for the specimens included in the database, should replicate that of concrete, whose value is not unique. Moreover, alkaline solutions present in the concrete fill its pores, which cover a small fraction of the concrete-bar contact surface, whereas in accelerated aging conditions bars are completely immersed in the alkaline solution that wets all the bar external surface. As in the case of elements immersed in water, the exposure to high temperatures to accelerate the alkali degradation process might affect the results. The thermal response of a structural member is a transient phenomenon influenced by many parameters, such as time-dependent solar radiation, temperature, wind speed fluctuations, material properties, surface characteristics, and section geometry [59]. Thermal analyses indicate that the design distributions are not likely to greatly exceed those provided by the New Zealand code [60] for any latitude between 45°S and 45°N, as the peak solar radiation levels on horizontal surfaces between these latitudes do not vary significantly. According to [60], the maximum temperature of reinforcing bars embedded within concrete never exceeds 45 °C. This thermal distribution is similar to that adopted by EN 1991-1-5 [61].

However, these considerations do not explain the dispersion of experimental results observed in Section 4. A possible reason may be the tensile test procedure adopted and, specifically, the anchorage system that should guarantee complete fiber tensile rupture (Section 2.1). Pictures of some failure modes were reported in the analyzed papers. Only few authors well-documented the failure mode observed providing photos and descriptions, whereas most of the papers provided only limited information.

Results included in the database were analyzed in terms of residual tensile strength. However, the tensile strength of the unconditioned control specimens varied significantly (see Section 3). Nowadays, good quality GFRP bars (with diameter between 10 mm and 28 mm) generally provide a tensile strength between 800 MPa and 1100 MPa (e.g. Ref. [28]). Two of the research groups declare strengths much lower than these values. The lowest strength is reported in Ref. [43] and refers to a group of specimens which strength ranges between 295 MPa and 407 MPa. The authors attributed this small strength “to a low fiber content as seen by SEM investigations”. The low unconditioned tensile strength values reported by Abbasi and Hogg [44], namely 362 MPa and 366 MPa, were attributed to the damage of fibers during the manufacturing process. The bad alignment of the fibers was excluded because straight glass fibers were observed after resin burning-off. Fiber damage, due to poor manufacturing, leads to inefficiency in the stress transfer mechanisms between fiber filaments, which causes a high strength reduction.

The tensile testing of GFRP bars is not an easy task with unconditioned specimens and becomes even more complex with conditioned bars. For example, in Ref. [62] the authors commented on the results of their tests by observing that “the conditioned GFRP bars usually failed at the end section of the conditioning zone (edges of the plastic reservoir). A sudden change in bar properties occurs here, which led to failure initiation. Therefore, the resulting failure stresses stand as a lower limit and would have been higher had the entire bar been subjected to the conditioning as in field situations”.

To overcome the issues associated with tensile testing, bending tests, usually with three-point bending test set-ups, were employed by some authors [35,63,64]. However, bending tests of GFRP bars do not allow for controlling the failure mode obtained. Specimens can fail due to fiber tensile rupture in the tension zone or to bar crushing in the compression zone.

The mechanism leading to failure is affected by the mechanical properties in compression and tension of the bar, which depend on the type of resin matrix and on the fiber volume fraction. Another important limit of bar bending tests is that the fibers of the outer (sleeve) layer, which are more degraded than inner (core) fibers in conditioned specimens, are the most stressed, whereas the core fibers, which retain their mechanical properties, provide a limited contribution to the bending strength. Local defects due to manufacture or handling can cause similar problems. On the other hand, a GFRP bar employed as internal reinforcement of a concrete slab subjected to bending can be assumed to be stressed in longitudinal direction homogeneously across its entire cross-section, which implies that core fibers play a primary role in the bar strength. Therefore, bending tests of reinforcing bars can provide strength values lower than those provided by the same bar subjected to real serviceability conditions.

Bending tests of concrete beams reinforced with GFRP bars, even if expensive, appear ideal for providing reliable results on the bar tensile strength since they do not require the development of a specific procedure or testing set-up and are the most realistic. However, results of these tests are affected by the mechanical properties of concrete, which vary over time and depend on the type of conditioning. This disadvantage can be solved by subjecting a series of concrete specimens, obtained from the same concrete batch used to cast the reinforced beam, to the same conditioning of the beam. These specimens should be then tested contemporarily to each bending test in order to measure the mechanical properties of concrete at that specific time. Nevertheless, the need to handle, condition, and test heavy and bulky specimens unfortunately make these tests much more expensive than bar tensile or bending tests.

6. Calibration of environmental reduction factors

In this section, the results collected in the database are statistically analyzed to calibrate environmental reduction factors that allow for obtaining the residual tensile strength of GFRP bars subjected to alkaline environment, salt solution, and immersed in water. Since bars exposed to hot air did not show a reduction of the tensile strength (Section 4.1), it was assumed that no environmental reduction factor is needed for this treatment. Furthermore, bars embedded within concrete beams were not considered in this section because limited results by only two research groups were found in the literature (Section 4.5).

To calibrate the environmental reduction factors, the "design by testing" procedure provided by EN 1990 [65] was followed. According to this procedure, the residual strength ratio σ_f/σ_{fu} can be expressed as:

$$\frac{\sigma_f}{\sigma_{fu}} = \gamma \cdot f(t,\xi) \tag{2}$$

where $f(t,\xi)$ is a deterministic function that relates the mean residual strength ratio $(\sigma_f/\sigma_{fu})_{avg}$ to the exposure time t and to relevant environmental parameters ξ, and γ is a normally-distributed unit-mean aleatoric function. As a first attempt, each exposure condition was analyzed separately for ranges *a* and *b*. Range *c* was not considered because degradation processes different from those of the exposure condition considered may arise with high temperatures, which in turn would affect the results obtained (see Section 5). Since exposure conditions and temperatures ranges were analyzed separately, the dependence of f to the environmental parameters ξ can be neglected, which provided $f(t,\xi) = f(t)$. As a first step, a linear shape of the function $f(t)$ was assumed:

Table 5
Results of the linear regression analysis for the different environmental conditions and ranges studied.

Range	Alkaline		Salt		Water	
	a	*b*	*a*	*b*	*a*	*b*
n	54	48	21	14	29	18
m	0.0002	−0.0007	0.0000	0.0005	0.0009	−0.0006
q	90.0083	90.2535	88.1377	84.8079	89.3492	89.9811
r^2	0.0058	0.0891	0.0000	0.2050	0.1275	0.0795

$$f(t) = mt + q \tag{3}$$

A linear regression analysis was performed on residual strength ratios in ranges *a* and *b* of specimens subjected to alkaline, salt, and water conditioning to obtain the parameters *m* and *q*. The results obtained are reported in Table 5, where r^2 is the coefficient of determination and *n* is the number of specimen of the specific range considered. It should be noted that specimens from Chen et al. [45] and Chen [46] were not included in the regression analysis of alkaline environment ranges because their results significantly differ from those of other authors for the same exposure condition (see Fig. 7a and b). Therefore, the number of specimens in ranges *a* and *b* of alkaline environment reduced from 66 to 54 and from 59 to 48, respectively. Although functions with more complex shapes (e.g. polynomial, exponential, etc.) provided results slightly more accurate than those obtained with Eq. (3), their behavior was not monotonical with time and therefore they were not considered.

In general, the slope *m* of the lines obtained from the linear regression analysis is very limited (Table 5). Furthermore, only ranges *b* of alkaline and water environments provided a negative slope, whereas all other ranges provided positive values of *m*, which would entail for an increase of the residual strength ratio with time. Therefore, it was assumed that the slope of the regression lines be negligible (i.e. $m \approx 0$) and *q* was computed as:

$$q = (\sigma_f/\sigma_{fu})_{avg} = 1/n \cdot \sum_{i=1}^{n} (\sigma_f/\sigma_{fu})_i \tag{4}$$

where $(\sigma_f/\sigma_{fu})_i$ is the residual strength ratio of the i-th specimen. Once the function $f(t)$ is known, γ can be obtained through the "design by testing" procedure proposed by EN 1990 [65]. To verify that γ is a unit-mean normally-distributed function for all ranges, the first four statistics moments, namely the average (μ), variance (s^2), skewness (γ_1), and kurtosis (γ_2), were computed for the γ functions associated with each range. In addition, the Kolgomorov-Smirnov (K-S) test was executed to verify the maximum distance between the γ function and a normal distribution with the same mean and standard deviation of the γ considered. The CoV of each γ function was computed too. The results obtained are reported in Table 6 for all ranges and exposure conditions considered.

Table 6 shows that all functions γ has mean values very close to unit and can be considered normally distributed. For comparison, the

Table 6
Results of the statistical analysis of the distribution of functions γ.

Range	Alkaline		Salt		Water	
	a	*b*	*a*	*b*	*a*	*b*
n	54	48	21	14	29	18
μ	1.009	1.010	1.005	1.002	1.006	1.006
s^2	0.011	0.011	0.005	0.003	0.006	0.007
γ_1	1.845	0.846	0.534	1.143	1.012	−0.051
γ_2	3.943	0.301	0.131	0.722	1.467	−0.440
CoV	0.104	0.103	0.070	0.053	0.080	0.082
K-S	0.182	0.125	0.133	0.199	0.188	0.111

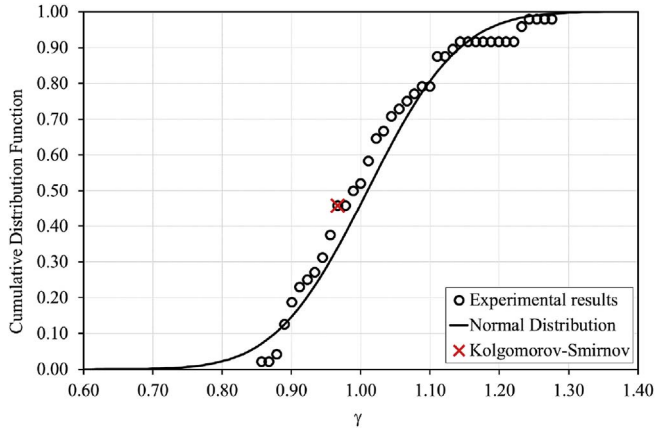

Fig. 17. Comparison between cumulative distribution frequencies of the experimental results of alkaline solution range *b* and corresponding normal distribution.

Table 7
Values of γ for the different environmental conditions and ranges studied.

Range	n		γ_m		γ_k		γ_d		Method
	a	*b*	*a*	*b*	*a*	*b*	*a*	*b*	
Alkaline	54	48	1.00	1.00	0.852	0.794	0.726	0.666	EN 1990 [65]
					0.849	0.791	0.713	0.650	t-distribution
Salt	21	14	1.00	1.00	0.884	0.902	0.783	0.828	EN 1990 [65]
					0.882	0.899	0.763	0.803	t-distribution
Water	29	18	1.00	1.00	0.873	0.802	0.738	0.781	EN 1990 [65]
					0.871	0.799	0.720	0.758	t-distribution

cumulative distribution function (CDF) of range *b* of alkaline environment, which is representative of the CDFs obtained, is compared with the CDF of the corresponding normal distribution in Fig. 17. The red cross mark reported in Fig. 17 represents the maximum difference between the two CDFs, as indicated by the K-S test of this range.

Since unit-mean can be assumed, a measure of the γ function accuracy in estimating the corresponding residual strength ratio can be obtained by the coefficients of variation (CoV). Table 6 reports relatively limited CoV values, which confirm the accuracy of the γ function provisions.

The characteristic (i.e. 5% percentile) value of the residual strength ratio $(\sigma_f/\sigma_{fu})_k$ can be obtained by Eq. (5) [65]:

$$(\sigma_f/\sigma_{fu})_k = (1 - k_n{\cdot}CoV)(\sigma_f/\sigma_{fu})_{avg} = \gamma_k(\sigma_f/\sigma_{fu})_{avg} \quad (5)$$

where k_n is the characteristic fractile factor, which depends on the number of test results *n* and is equal to 1.64 for an infinite number of measures. EN 1990 [65] provides also a procedure for direct assessing the design value $(\sigma_f/\sigma_{fu})_d$ for ultimate limit state verifications:

$$(\sigma_f/\sigma_{fu})_d = (1 - k_{d,n}{\cdot}CoV)(\sigma_f/\sigma_{fu})_{avg} = \gamma_d(\sigma_f/\sigma_{fu})_{avg} \quad (6)$$

where $k_{d,n}$ is the design fractile factor, which is associated with a probability of 0.12%, depends on the number of test results *n*, and is equal to 3.04 for an infinite number of measures. Mean (γ_m), characteristic (γ_k), and design (γ_d) values of γ obtained are reported in Table 7.

In addition, values of γ associated with a 5% (characteristic value) and 0.12% (design value) probability of obtaining a lower value [65] were computed based on the Student's t-distribution. The results obtained, which are provided in Table 7, are similar to those based on the procedure by EN 1990 [65] for ranges with large number of specimens and are more conservative when *n* decreases.

The characteristic and design values of the residual strength ratio computed by Eqs. (5) and (6), respectively, are reported in Table 8 for each range studied. Residual strength ratios provided in Table 8 are depicted in Figs. 7, 10 and 13 for bars exposed to alkaline environment, salt solution, and immersed in water, respectively.

The residual tensile strength of a GFRP bar exposed to an alkaline environment, salt solution, or immersed in water at a temperature within ranges *a* and *b* can be obtained as:

$$\sigma_{f,p} = \sigma_{fu}\left[\gamma_p(\sigma_f/\sigma_{fu})_{avg}\right] \quad (7)$$

where $p = m$, k, and d for mean, characteristic, and design values, respectively. Since environmental reduction factors η_a are generally multiplied by the unconditioned bar tensile strength σ_{fu} to obtain the reduced tensile strength (see e.g. Ref. [23]), results reported in Table 8 represent environmental reduction factors η_a.

Environmental reduction factors provided by ACI 440.1R-15 [23] and CNR-DT 203/2006 [26] are equal to 0.8 for concrete elements not exposed to earth and weather and to 0.7 for concrete elements exposed to earth and weather. These factors, which include the effect of temperature on the rebar (provided that the service temperature is lower than the matrix resin glass transition temperature), represent conservative estimates based on the consensus of the guideline committees. The most conservative values of η_a obtained in this paper following EN 1990 [65] are equal to 0.61 and 0.67 for specimens in alkaline environment and conditioned at temperatures in ranges *a* and *b*, respectively (Table 8). However, results of specimens exposed to alkaline environments discussed in Section 4.2 were mostly obtained by direct exposure of the GFRP bars to alkaline solutions, which are likely to provide a higher degradation than that of bars embedded in concrete and exposed to alkaline environments (see Section 5). Values of η_a obtained for each exposure condition analyzed at environmental temperature (range *a*) are all close to 0.8, which is consistent with values of η_a provided by Refs. [23,26] for concrete elements not exposed to earth and weather.

The reliability of the η_a calibrated in this paper is strictly related to the number of tests considered and to the homogeneity of results in each range [65]. However, in some cases significant discrepancies between results with similar environmental conditions by different research groups were observed (Sections 4 and 5). Further studies involving concrete elements reinforced with GFRP bars and exposed to real environmental conditions are needed to provide more reliable estimation of the composite durability.

Table 8
Residual strength ratios [%] obtained from the statistical analysis for the different environmental conditions and ranges studied.

Range	n		$\gamma_m(\sigma_f/\sigma_{fu})_{avg}$		$\gamma_k(\sigma_f/\sigma_{fu})_{avg}$		$\gamma_d(\sigma_f/\sigma_{fu})_{avg}$		Method
	a	*b*	*a*	*b*	*a*	*b*	*a*	*b*	
Alkaline	54	48	91.65	86.56	78.09	72.77	66.51	61.00	EN 1990 [65]
					77.81	72.46	65.31	59.60	t-distribution
Salt	21	14	88.18	87.02	77.98	79.57	69.00	72.99	EN 1990 [65]
					77.74	79.30	67.24	70.82	t-distribution
Water	29	18	93.45	87.32	81.56	74.96	69.00	72.99	EN 1990 [65]
					81.43	74.71	67.24	70.82	t-distribution

7. Conclusions

In this paper, the residual strength ratio of GFRP bars subjected to different environment conditioning was investigated in an attempt to shed light on the durability of this reinforcement that can promisingly increase the durability of reinforced concrete structures. 356 tensile tests on conditioned GFRP bars were collected from the literature and their results were analyzed and compared. A statistical analysis of the results was carried out following the "design by testing" procedure provided by EN 1990. Characteristics and design environmental reduction factors were provided for specimens subjected to alkaline environment, salt solution, and immersed in water. Based on the results obtained, the following conclusions can be drawn:

- significant differences of methodologies, procedures, and result interpretation between different experimental studies with similar environmental conditions were observed. The differences in testing procedures can explain the dispersion of the results.
- environmental reduction factors obtained are very similar to those provided by ACI 440.1R-15 and CNR-DT 203/2006 for all exposure conditions studied at environmental temperature. Lower values of η_a were obtained for specimens exposed to temperature higher than 25 °C.
- a shared standard procedure is urgently needed. Such procedure should guarantee the effectiveness and reliability of the test set-up - with particular attention to anchoring and possible damage of the bar - and the application of environmental conditions that correctly reproduce real field conditions without introducing further deterioration sources. Namely, durability tensile tests on GFRP bars should comply with the following rules: i) tests in the alkaline environment should be carried out on specimens comprised by GFRP bars embedded within concrete (dry or wet) whereas direct bar exposure to alkaline solutions should be avoided; ii) the exposure temperature should not exceed 45 °C and 40 °C for alkaline environments and water solutions, respectively; iii) fiber tensile rupture, proved by photos of the failed specimens, should be obtained.

Although the large number of collected test results, the significant discrepancies observed between the results suggests the need of further studies involving concrete elements reinforced with GFRP bars and exposed to real environmental conditions to provide more reliable estimation of the composite durability.

List of symbols

*	bars embedded within concrete or mortar.
AR	AR-glass
E	E-glass
E-CR	corrosion resistant E-glass
E-VE	epoxy vinylester
FT	freeze and thaw cycles
M	molded
M-VE	modified vinylester
PE	polyester
PT	polyethylene terephthalate
R	ribbed with glass fiber wrapped around the bar longitudinal axis
Rsa	R + Sa
S	smooth
Sa	sand-coated
TP	thermoplastic
UM-VE	urethane modified vinylester
VE + PE	mixed vinylester and polyester
VE	vinylester
WD	wet and dry cycles

Appendix A. Supplementary data

Supplementary data related to this article can be found at http://dx.doi.org/10.1016/j.compositesb.2017.12.037.

References

[1] Klowak C, Memon A, Mufti A. Static and fatigue investigation of second generation steel-free bridge decks. Cement Concr Compos 2006;28:890–7.
[2] Mufti A, Neale K. State-of-the-art of FRP and SHM applications in bridge structures in Canada. Compos Res J 2008;2(2):60–9.
[3] Rostàsy F. FRP tensile elements for prestressed concrete: state of the art, potentials and limits. In: Nanni A, Dolan C, editors. Fiber-reinforced plastic reinforcement for concrete structures - SP-138. Farmington Hills, Mich: American Concrete Institute; 1993. p. 347–65.
[4] Carvelli V, Pisani M, Poggi C. Fatigue behaviour of concrete bridge deck slabs reinforced with GFRP bars. Compos Part B 2010;41:560–7.
[5] D'Antino T, Carloni C, Sneed LH, Pellegrino C. Fatigue and post-fatigue behavior of PBO FRCM-concrete joints. Int J Fatig 2015;81:91–104.
[6] D'Antino T, Triantafillou TC. Accuracy of design-oriented formulation for evaluating the flexural and shear capacities of FRP-strengthened RC beams. Struct Concr 2016;17(3):425–42.
[7] D'Antino T, Pisani MA. Evaluation of the effectiveness of current guidelines in determining the strength of RC beams retrofitted by means of NSM reinforcement. Compos Struct 2017;167:166–77.
[8] Del Zoppo M, Di Ludovico M, Balsamo A, Prota A, Manfredi G. FRP for seismic strengthening of shear controlled RC columns: experience from earthquakes and experimental analysis. Compo Part B 2017;129:47–57.
[9] Rousakis TC, Saridaki ME, Mavrothalassitou SA, Hui D. Utilization of hybrid approach towards advanced database of concrete beams strengthened in shear with FRPs. Compos Part B 2016;85:315–35.
[10] Seo S-Y, Sung Lee M, Feo L. Flexural analysis of RC beam strengthened by partially de-bonded NSM FRP strip. Compos Part B 2016;101:21–30.
[11] Charalambidi BG, Rousakis TC, Karabinis AI. Analysis of the fatigue behavior of reinforced concrete beams strengthened in flexure with fiber reinforced polymer laminates. Compos Part B 2016;96:69–78.
[12] Di Luccio G, Michel L, Ferrier E, Martinelli E. Seismic retrofitting of RC walls externally strengthened by flax–FRP strips. Compos Part B 2017;127:133–49.
[13] Triantafillou GG, Rousakis TC, Karabinis AI. Analytical assessment of the bearing capacity of RC beams with corroded steel bars beyond concrete cover cracking. Compos Part B 2017;119:132–40.
[14] Kalfat R, Al-Mahaidi R. Mitigation of premature failure of FRP bonded to concrete using mechanical substrate strengthening and FRP spike anchors. Compos Part B 2016;94:209–17.
[15] Carozzi FG, Bellini A, D'Antino T, de Felice G, Focacci F, Hojdys L, et al. Experimental investigation of tensile and bond properties of Carbon-FRCM composites for strengthening masonry elements. Compos Part B 2017;128:100–19.
[16] D'Antino T, Papanicolaou C. Mechanical characterization of textile reinforced inorganic-matrix composites. Compos Part B 2017;127:78–91.
[17] Daniel I, Ishai O. Engineering mechanics of composite materials. second ed. New York: Oxford University Press; 2006. p. 411.
[18] Karbhari VM, Murphy K, Zhang S. Effect of concrete based alkali solutions on short-term durability of e-glass/vinyl ester composites. J Compos Mater 2002;36(17):2101–21.
[19] fib (International Federation for StrucConcrete). FRP reinforcement in RC structures. Lausanne: fib; 2007. p. 120.
[20] Yan F, Lin Z, Zhang D, Gao Z, Li M. Experimental study on bond durability of glass fiber reinforced polymer bars in concrete exposed to harsh environmental agents: freeze-thaw cycles and alkaline-saline solution. Compos Part B 2017;116:406–21.
[21] Benmokrane B, Ali AH, Mohamed HM, ElSafty A. Laboratory assessment and durability performance of vinyl-ester, polyester, and epoxy glass-FRP bars for concrete structures. Compos Part B 2017;114:163–74.
[22] ACI 549.4R-13. Guide to design and construction of externally bonded fabric-reinforced cementitious matrix (FRCM) systems for repair and strengthening concrete and masonry structures. Farmington Hills, MI: American Concrete Institute; 2013. p. 71.
[23] ACI 440.1R-15. Guide for the design and construction of concrete reinforced with FRP bars. Farmington Hills, MI: American Concrete Institute; 2015. p. 88.
[24] Carvelli V, Pisani M, Poggi C. High temperature effects on concrete members reinforced with GFRP rebars. Compos Part B 2013;54:125–32.
[25] Japan Society of Civil Engineers (JSCE). Recommendation for design and construction of concrete structures using continuous fiber reinforcing materials. 1997. Tokyo.
[26] CNR-DT 203/2006. Guide for the design and construction of concrete structures reinforced with fiber-reinforced polymer bars. Rome: National Research Council; 2006. p. 35.
[27] CAN/CSA-S806-02. Design and construction of building components with fibre-reinforced polymers. Rexdale: Canadian Standards Association; 2012. p. 198.
[28] Carvelli V, Fava G, Pisani M. Anchor system for tension testing of large diameter GFRP bars. ASCE J Compos Construct 2009;13(5):344–9.
[29] ASTM D7205/D7205M-6. Standard test method for tensile properties of fiber reinforced polymer matrix composite bars. West Conshohocken, PA: ASTM International; 2016. p. 13.
[30] ASTM E 632-82. Standard practice for developing accelerated tests to aid prediction

of the service life of building components and materials. West Conshohocken, PA: ASTM International; 1996. p. 6.
[31] Vijay P. Aging and design of concrete members reinforced with GFRP bars PhD Thesis Morgantown, West Virginia, USA: Department of Civil Engineering, West Virginia University; 1999 p. 205.
[32] ASTM E 2041-03. Standard method for estimating kinetic parameters by differential scanning calorimeter using the Borchardt and Daniels method. West Conshohocken, PA: ASTM International; 2003. p. 9.
[33] ASTM E 698-01. Standard test method for Arrhenius kinetic constants for thermally unstable materials using differential scanning calorimetry and the Fkynn/Wall/Ozawa method. West Conshohocken, PA: ASTM International; 2005. p. 8.
[34] Davalos J, Chen Y, Ray I. Long-term durability prediction models for GFRP bars in concrete environment. J Compos Mater 2012;46(16):1899–914.
[35] Gonenc O. Durability and service life prediction of concrete reinforcing materials PhD Thesis Madison, WI, USA: Department of Civil and Environmental Engineering,University od Wisconsin-Madison; 2003
[36] Boris T, Porter M. Advancements in GFRP materials provide improved durability for reinforced concrete. Convention, Marketing/technical sessions of the Composites Institute's international composites EXPO '99, Cincinnati, OH, USA. 1999.
[37] Tannous FE, Saadatmanesh H. Durability of AR glass fiber reinforced plastic bars. J Compos Construct 1999;3(1):12–9.
[38] Bhise VS. Strength degradation of GFRP bars PhD Thesis Blacksburg, Virginia, USA: Department of Civil and Environmental Engineering, Virginia Polytechnic and State University; 2002 p. 105.
[39] Almusallam T, Al-Salloum Y, Alsayed S, Alhozaimy A. Durability of GFRP rebars in stressed concrete beams at different environments. The 6th Saudi engineering conference. Dhahran, Saudi Arabia: KFUPM; 2002.
[40] Al-Zahrani MM, Al-Dulaijan SU, Sharif A, Maslehuddin M. Durability performance of glass fiber reinforced plastic reinforcement in harsh environments. The 6th Saudi engineering conference. Dhahran, Saudi Arabia: KFUPM; 2002.
[41] Stone DK, Koenigsfeld D, Myers J, Nanni A. Durability of GFRP rods, laminates and sandwich panels subjected to various environmental conditioning. Second international conference on durability of fiber reinforced polymer (FRP) composites for construction, Montreal, Quebec, Canada. 2002.
[42] Gaona FA. Characterization of design parameters for fiber reinforced polymer composite reinforced concrete systems PhD Thesis College Station, TX, USA: Zachry Department of Civil Engineering, Texas A&M University; 2003 p. 270.
[43] Micelli F, Nanni A. Durability of FRP rods for concrete structures. Construct Build Mater 2004;18:491–503.
[44] Abbasi A, Hogg PJ. Temperature and environmental effects on glass fibre rebar: modulus, strength and interfacial bond strength with concrete. Compos Part B 2005;36:394–404.
[45] Chen Y, Davalos JF, Ray I. Durability prediction for GFRP reinforcing bars using short-term data of accelerated aging tests. J Compos Construct 2006;10(4):279–86.
[46] Chen Y. Accelerated ageing tests and long-term prediction models for durability of FRP bars in concrete PhD Thesis Morgantown, West Virginia, USA: Department of Civil and Environmental Engineering, West Virginia University; 2007 p. 214.
[47] Won J, Lee S, Kim Y, Jang C, Lee S. The effect of exposure to alkaline solution and water on the strength–porosity relationship of GFRP rebar. Compos Part B 2008;39:764–72.
[48] Kim H, Park Y, You Y, Moon C. Short-term durability test for GFRP rods under various environmental conditions. Compos Struct 2008;83:37–47.
[49] Robert M, Cousin P, Benmokrane B. Durability of GFRP reinforcing bars embedded in moist concrete. J Compos Construct 2009;13(2):66–73.
[50] Almusallam TH, Al-Salloum YA, Alsayed SH, El-Gamal S, Aqel M. Tensile properties degradation of glass fiber-reinforced polymer bars embedded in concrete under severe laboratory and field environmental conditions. J Compos Mater 2012;47(4):393–407.
[51] Al-Salloum YA, El-Gamal S, Almusallam TH, Alsayed SH, Aqel M. Effect of harsh environmental conditions on the tensile properties of GFRP bars. Compos Part B 2013;45:835–44.
[52] Robert M, Benmokrane B. Combined effects of saline solution and moist concrete on long-term durability of GFRP reinforcing bars. Construct Build Mater 2013;38:274–84.
[53] Sawpan MA, Mamun AA, Holdsworth PG. Long term durability of pultruded polymer composite rebar in concrete environment. Mater Des 2014;57:616–24.
[54] Smith R, Purnama A, Al-Barwani HH. Sensitivity of hypersaline Arabian Gulf to seawater desalination plants. Appl Math Model 2007;31:2347–54.
[55] Taher MM, Mohamed ARM, Al-Ali AKH. Some ecological characteristics and ichthyofauna of surrounding Sammaliah Island, Abu Dhabi, UAE. Bahamas J Sci 2012;30(2):31–49.
[56] John VC, Coles SL, Abozed A i. Seasonal cycles of temperature,salinity and water masses of the Western Arabian Gulf. Oceanol Acta 1990;13(3):273–82.
[57] Robert M, Wang P, Cousin P, Benmokrane B. Temperature as an accelerating factor for long-term durability testing of FRPs: should there be any limitations? ASCE J Compos Construct August 2010;14(4):361–7.
[58] Kabiri K, Pradhan b, Rezai H, Ghobadi Y, MM. Fluctuation of sea surface temperature in the Persian Gulf and its impact on coral reef communities around Kish Island. IEEE colloquium on humanities, science & engineering research (CHUSER 2012), Kota Kinabalu, Sabah, Malaysia. 2012.
[59] Priestley M. Chapter 5: the thermal response of concrete bridges. In: Cope RJ, editor. Concrete bridges engineering: performance and advances. London (UK): Elsevier Applied Science; 1978. p. 143–88.
[60] N. Z. Ministry of Work and Development. Highway bridge design brief, CDP701/A. 1978.
[61] European Committee for Standardization (CEN). Eurocode 1: actions on structures - Part 1-5: general actions - thermal actions. EN 1991-1-5. Brussels: CEN; 2009.
[62] Debaiky A, Nkurunziza G, Benmokrane B, Cousin P. Residual tensile properties of GFRP reinforcing bars after loading in severe environments. ASCE J Compos Construct 2006;10(5):370–80.
[63] Gentry TR, Bank LC, Barkatt A, Prian L. Accelerated test methods to determine the long-term behavior of composite highway structures subject to environmental loading. J Compos Technol Res 1998;20(1):38–50.
[64] Robert M, Benmokrane B. Behavior of GFRP reinforcing bars subjected to extreme temperatures. J Compos Construct 2010;14(4):353–60.
[65] European Committee for Standardization (CEN). Eurocode - basis of structural design. EN 1990. Brussels: CEN; 2002.